

Distinct age dependent C fibre driven oscillatory activity in the rat somatosensory cortex

<https://doi.org/10.1523/ENEURO.0036-20.2020>

Cite as: eNeuro 2020; 10.1523/ENEURO.0036-20.2020

Received: 31 January 2020

Revised: 3 July 2020

Accepted: 27 July 2020

This Early Release article has been peer-reviewed and accepted, but has not been through the composition and copyediting processes. The final version may differ slightly in style or formatting and will contain links to any extended data.

Alerts: Sign up at www.eneuro.org/alerts to receive customized email alerts when the fully formatted version of this article is published.

Copyright © 2020 Chang et al.

This is an open-access article distributed under the terms of the Creative Commons Attribution 4.0 International license, which permits unrestricted use, distribution and reproduction in any medium provided that the original work is properly attributed.

1
2
3
4
5
6
7
8
9
10
11
12
13
14
15
16
17
18
19
20
21
22
23
24
25
26
27
28
29
30
31
32
33

Manuscript Title

Distinct age dependent C fibre driven oscillatory activity in the rat somatosensory cortex

Abbreviated Title: C fibre activation of adult and juvenile S1 cortex

Pishan Chang, Lorenzo Fabrizi and Maria Fitzgerald

Department of Neuroscience, Physiology & Pharmacology, University College London, Gower Street,
London WC1E6BT, United Kingdom

Author Contributions: PC and MF Designed research, PC Performed research, PC, LF and MF
Analyzed data, PC, LF and MF Wrote the paper.

Correspondence should be addressed to: Professor Maria Fitzgerald, m.fitzgerald@ucl.ac.uk

Number of Figures: 6

Number of Tables: 0

Number of words for Abstract: 249

Number of words for Significance Statement: 70

Number of words for Introduction 646

Number of words for Discussion:1713

Acknowledgements: This research was supported by grants from the Medical Research Council
(G0901269 MF) and BBSCRC (BB/R00823X/1, MF & PC). LF is a Medical Research Council Career
Development Fellow (MR/L019248/1).

Conflict of Interest: Authors report no conflict of interest

Funding sources: Medical Research Council (G0901269, MR/L019248/1) and BBSCRC
(BB/R00823X/1).

34 **Distinct age dependent C fibre driven oscillatory activity in the rat somatosensory**
35 **cortex**

36

37

38

39

40 **Abbreviated Title:** C fibre activation of adult and juvenile S1 cortex

41

42

Abstract

When skin afferents are activated, the sensory signals are transmitted to the spinal cord and eventually reach the primary somatosensory cortex (SI), initiating the encoding of the sensory percept in the brain. While subsets of primary afferents mediate specific somatosensory information from an early age, the subcortical pathways that transmit this information undergo striking changes over the first weeks of life, reflected in the gradual emergence of specific sensory behaviours. We therefore hypothesised that this period is associated with differential changes in the encoding of incoming afferent volleys in SI. To test this, we compared SI responses to A fibre skin afferent stimulation and A+C skin afferent fibre stimulation in lightly anaesthetised male rats at postnatal day (P) 7, 14, 21 and 30. Differences in SI activity following A and A+C fibre stimulation changed dramatically over this period. At P30, A+C fibre stimulation evoked significantly larger gamma, beta and alpha energy increases compared to A fibre stimulation alone. At younger ages, the changes in S1 oscillatory activity evoked by the two afferent volleys were not significantly different. Silencing TRPV1+ C fibres with QX-314 significantly reduced the gamma and beta SI oscillatory energy increases evoked by A+C fibres, at P30 and P21, but not at younger ages. Thus, C fibres differentially modulate SI oscillatory activity only from the third postnatal week, well after the functional maturation of the somatosensory cortex. This age-related change in afferent evoked S1 oscillatory activity may underpin the maturation of sensory discrimination in the developing brain.

Significance Statement

Behavioural responses to sensory stimulation of the skin undergo major developmental changes over the first postnatal weeks. Here we show that this is accompanied by a shift in the differential frequency encoding of sensory A fibre and C fibre afferent inputs into the developing rat somatosensory cortex. The results demonstrate major postnatal changes in the ability of the cortex to differentiate between afferent sensory inputs arriving in the mammalian brain.

Introduction

Distinct temporal rhythms of neural activity are an essential part of communication in the brain. In both humans and rodents, tactile and nociceptive sensory stimulation is associated with alterations in these patterns (Peng and Tang, 2016; Pfurtscheller and Lopes da Silva, 1999; Stančák, 2006). The primary somatosensory cortex (S1) plays a key role in perceptual recognition of the presence, location, intensity, submodality and quality of touch, thermal sensibility, and pain (Vierck et al., 2013) and the oscillatory rhythms commonly recorded over the rat somatosensory cortex (S1) are selectively modified by sensory stimulation. For example, the amplitudes of both alpha and beta rhythms in rat S1 are suppressed by a tactile stimulus, with a comparable time course to humans (Fransen et al., 2016) and noxious skin stimulation results in selective increases in S1 gamma activity in both rodents and human subjects (Hu and Iannetti, 2019). Gamma activity reflects stimulus encoding in S1 (Yue et al., 2020) and experimental induction of S1 gamma oscillations via optogenetic activation of parvalbumin-expressing inhibitory interneurons enhances nociceptive sensitivity and induces aversive avoidance behaviour (Tan et al., 2019). Changes in other oscillatory frequencies are also reported following skin stimulation, including decreases in alpha and beta energy related to cutaneous stimulus intensity (Nickel et al., 2017) and synchronization of theta-alpha energy following noxious stimulation (Peng et al., 2018). The ability of particular modalities of afferent input to differentially modulate the temporal rhythms in S1 may be an important mechanism underpinning the communication of sensory discrimination in the brain.

Behavioural reflex recording in newborn rodents and humans reveal that somatosensory discrimination is poorly developed such that 'nociceptive' reflexes are indistinguishable from those evoked by innocuous touch (Cornelissen et al., 2013; Fitzgerald et al., 1988; Green et al., 2019). The underlying modality specific connections in the spinal cord also develop postnatally, characterised by structural and functional refinement of A fibre terminals and their synaptic inputs (Beggs et al., 2002; Coggeshall et al., 1996; Fitzgerald and Jennings, 1999; Granmo et al., 2008), gradual strengthening of C fibre synaptic connections (Baccei et al., 2003; Fitzgerald, 2005; Walker et al., 2007) and maturation of dorsal horn inhibitory circuitry (Baccei and Fitzgerald, 2004; Koch et al., 2012), accompanied by the onset of selective descending brainstem control of A and C fibre evoked (Koch and Fitzgerald, 2014) and tactile and noxious evoked (Schwaller et al., 2017) dorsal horn activity, all of which accompany the segregation of innocuous and noxious cutaneous reflexes over the postnatal period (Baccei and Fitzgerald, 2013).

The delayed postnatal emergence of modality selective dorsal horn circuitry is likely to impact upon the sensory modulation of oscillatory rhythms in S1. Indeed there is evidence in human infants of a transition in brain response following tactile and noxious stimulation from nonspecific, evenly dispersed neuronal bursts to modality-specific, localized, evoked potentials, suggesting an emergence of specific neural circuits necessary for discrimination between touch and nociception (Fabrizi et al., 2011). Temporal patterns of cortical communication develop gradually in rodents over the first postnatal weeks (Khazipov et al. 2004; Minlebaev et al. 2011, Mitrukhina et al. 2015, Chang et al., 2016a) but the maturation of selective modification of these rhythms by different afferent inputs is not known.

We hypothesised that the first postnatal weeks are associated with changes in the encoding of incoming afferent volleys in S1 and specifically that myelinated A fibre and unmyelinated C fibre cutaneous afferents only differentially modulate S1 oscillatory activity after two postnatal weeks. To test this, we compared the effect of A fibre and C fibre skin afferent fibre stimulation upon S1 oscillatory activity in lightly anaesthetised male rats at postnatal day (P) 7, 14, 21 and 30. S1 evoked potentials and oscillatory rhythms were recorded at each age, and the ability of C fibre versus A fibre

118 cutaneous afferent input to differentially modulate the temporal rhythms in S1 was evaluated by
119 activation or selective silencing techniques.

120

121

122 **Materials and Methods**

123 **Animals and Ethics**

124 All experiments were performed in accordance with the United Kingdom Animal (Scientific
125 Procedures) Act 1986. Reporting is based on the ARRIVE Guidelines for Reporting Animal Research
126 developed by the National Centre for Replacement, Refinement and Reduction of Animals in
127 Research, London, United Kingdom. Male Sprague-Dawley rats aged postnatal day (P) 7, 14, 21 and
128 30, were obtained from the Biological Services Unit, XXXXXXXXXXXX. Rats were housed in controlled
129 conditions in accordance with guidance issued by the Medical Research Council in Responsibility in
130 the Use of Animals for Medical Research (1993) and all experiments were carried out under Licence
131 from the UK Home Office and with Local Ethical Review panel approval. All animals were from the
132 same colony, bred and maintained in-house, and exposed to the same caging, diet and handling
133 throughout development. Rats were housed in cages of four age-matched animals (P30) or with the
134 dam and littermates (P7, 14 and 21) under controlled environmental conditions (24–25°C; 50–60%
135 humidity; 12 h light/dark cycle) with free access to food and water. Animals of both sexes were
136 randomly picked from litters for recording. Treatment groups were distributed across multiple litters
137 and/or adult cage groups.

138 **Recording from the primary somatosensory cortex (S1)**

139 Electrophysiological recordings were conducted under general anaesthesia. Rats were initially
140 anaesthetised with 4% isoflurane (Abbot, AbbVie Ltd., Maidenhead, United Kingdom) in 100% O₂
141 (flow rate of 1-1.5 litre/min) and trachea cannulated (P7: 27 gauge; P14: 18 gauge; P21: 18 gauge;
142 P30: 16 gauge). They were then placed in a stereotaxic frame and the cannula connected immediately
143 to a mechanical ventilator (Bioscience, Kent, UK) and calibrated isoflurane vaporizer (Harvard
144 Apparatus, Cambridge, MA). Anaesthesia was adjusted to 2-3 % isoflurane in 100 % O₂ (1-1.5
145 litre/min) and a craniotomy performed to expose the surface of the cerebral cortex. Body
146 temperature was maintained with a thermostatically controlled heated blanket and the
147 electrocardiogram was monitored throughout (Neurolog, Digitimer, Welwyn Garden City, UK). A
148 recording electrode (stainless steel 25 mm, E363/1, Plastics One Inc. Virginia, USA) was inserted into
149 the primary somatosensory cortex in the somatotopic region for the hindpaw. Coordinates for P7
150 and P14 rats were lateral 2.0 mm from midline and posterior 0.5 mm from the bregma; and for P21
151 and P30 rats were lateral 2.5 mm from midline, and posterior 1 mm from the bregma (Kalliomäki et
152 al., 1993; Paxinos and Watson, 2013; Paxinos et al., 2013). The reference electrode was placed
153 subcutaneously on the surface of the skull anterior to the bregma, and the ground electrode was
154 placed subcutaneously in the back. The depth of the recording electrode was adjusted to optimize
155 the evoked potential (EP) amplitude and the recording depth verified histologically to be in layer 5 to
156 6 of the somatosensory cortex as described previously (Chang et al., 2016b). The isoflurane
157 concentration was then reduced to 1% and allowed to equilibrate for at least 30 minutes before
158 recording began. Continuous activity was recorded under 1% isoflurane using a Neurolog NL100
159 headstage connected to a NL104 amplifier and a low pass NL125 filter (100 Hz). The signal was
160 sampled at 16K Hz using Axon Instruments (Digidata 1400A, Molecular Devices, Sunnyvale, CA). Data

was acquired and stored using a Windows PC based programme, WinEDR v3.3.6 (John Dempster, University of Strathclyde, United Kingdom) for later analysis.

The recording parameters were confirmed in P30 animals by recording LFP following plantar hindpaw electrical stimulation under 1% isoflurane. Clear EPs were recorded following contralateral, but not ipsilateral hindpaw stimulation, consistent with previous studies (Killackey, 1973; Welker, 1971). Increasing current intensity (500 μ s square pulses of 3.2 μ A, 32 μ A, 320 μ A, 3.2 mA; 10 stimuli with a 10 sec inter-stimulus interval (ISI) in n=6 animals) established the threshold required to elicit optimal evoked potentials in S1 to be 3.2 mA at P30.

Hindpaw skin stimulation

Electrical stimulation was applied through two stainless steel pin electrodes placed subcutaneously 3-5 mm apart in the plantar skin of the contralateral hindpaw, using a constant current stimulator (Neurolog, Digitimer, Welwyn Garden City, UK). Different pulse widths were used to recruit the following afferent fibre groups: A β and A δ fibres (50 μ s, 3.2 mA) or A β , A δ and C-fibres (500 μ s, 3.2 mA) (Jennings and Fitzgerald, 1998; Koch and Fitzgerald, 2014). Stimuli were applied with a 10 sec ISI, 10 times at A fibre intensity and 10 times at A + C fibre intensity, separated by an interval of 5 minutes. The afferent groups excited by these peripheral electrical stimulation intensities, have been previously established from recording nerve compound action potentials (Koch and Fitzgerald, 2014) and for simplicity and clarity are denoted 'A fibre' and 'A+C fibre' stimulation intensities throughout.

C-fibre silencing

C-fibres were silenced using a combination of QX-314 and capsaicin, which effectively blocks action potential generation by insertion of the membrane impermeable sodium channel blocker QX-314 into C fibre afferents via the TRPV1 channel pore (Binshtok et al., 2007; Puopolo et al., 2013). The combination of QX-314 (lidocaine N-ethyl bromide) (2%, Tocris Bioscience, Bristol, UK) and capsaicin (0.1%, Sigma, Dorset, UK) with solvent (20% ethanol, 7% Tween 80, and 70% normal saline) was prepared and stored at -20 °C and injected into the plantar hindpaw (P14: 5 μ l; P21 and P30: 10 μ l).

The effectiveness of C fibre block on heat and mechanical nociception was tested at P14, 21 and P30. For heat nociception we used the Hargreaves test in awake animals, while for mechanical nociception we measured the EMG of the withdrawal reflex to plantar pinch in lightly anaesthetised animals (1% isoflurane). QX-314/capsaicin caused an increase in withdrawal latency to heat stimulation compared to baseline, peaking at 60-150 minutes after injection and lasting over 3 hours. Friedman test with Dunn's multiple comparisons test (n=8 at all ages): $\chi^2(6)$ at P14 = 19.02 (p = 0.004); $\chi^2(6)$ at P21 = 26.46 (p < 0.001); $\chi^2(6)$ at P30 = 25.82 (p < 0.001)). QX-314/capsaicin also caused a significant decrease in EMG amplitude to pinch peaking between 60-150 minutes (Wilcoxon test (n=8 at all ages): W at P30 = -36 (p = 0.008); W at P21 = -45 (p = 0.004); W at P14 = -36 (p = 0.008)).

Experimental Design and Statistical Analysis

a. Time domain analysis

Peak EP amplitude and onset latency for each animal/condition were measured following electrical stimulation. Continuous recordings were segmented into epochs of 1.5 seconds, from 0.15 sec pre-stimulus to 1.35 sec post-stimulus. Epochs were then baseline corrected and averaged for each animal (10 stimuli per animal) and peak EP amplitudes identified.

b. Frequency domain analysis

Energy changes in LFP in different frequency bands were calculated using the Hilbert transform in the Brainstorm MATLAB toolbox (Bruns, 2004; Le Van Quyen et al., 2001; Tadel et al., 2011). This filters the signals in various frequency bands with a band-pass filter and then computes the Hilbert transform of the filtered signal. The magnitude of the Hilbert transform of a narrow-band signal is a measure of the envelope of this signal, and therefore gives an indication of the activity in this frequency band. Energy was then calculated by squaring the magnitude of the Hilbert transform. Continuous recordings were segmented into 10 seconds epochs, from 5 sec pre-stimulus to 5 sec post-stimulus. Each epoch was then filtered in various frequency bands with band-pass filters for delta (2-4 Hz), theta (5-7 Hz), alpha (8-12 Hz), beta (15-29 Hz), and gamma (30-90 Hz) band. The Hilbert transform of each filtered signal was then computed and averaged within time bins of 0.5 seconds (0-500, 500-1000 and 1000-1500 ms post-stimulus). These were then averaged across repetitions within each animal. Stimulus-induced energy changes for each animal were then calculated by normalising the post-stimulus values by a baseline time bin which did not include a spontaneous activity burst (which may have occurred just before the stimulus). Stimulus-induced energy changes specifically associated with C fibre recruitment were estimated by comparing energy changes following A+C vs A fibre stimulation (A+C/A ratio). We then estimated the stimulus-induced energy changes following A+C stimulation before and 60-150 min after administration of QX-314/capsaicin and compared them (A+C after-/before-QX-314 ratio) to identify changes in activity patterns caused by the silencing of C fibres.

c. Statistical Analysis

Statistical analysis of EP peak amplitude, onset latency and energy changes was performed using Graphpad Prism 6 (GraphPad Software, CA, USA) and MATLAB. All data are presented as mean \pm SEM. Mean peak EP amplitude and onset latency were compared across ages and stimulus intensities (condition) with a two-way mixed ANOVA (within-subjects: stimulus intensity (condition); between-subjects: age) followed by Tukey's multiple comparisons test.

Paired differences in energy from (i) A+C fibre vs A fibre stimulation and (ii) after vs. before QX314 treatment were computed for each frequency band and post-stimulus time bin, at each age. These differences were statistically analysed using estimation statistics, reporting mean differences (effect size) with expressions of uncertainty (confidence interval estimates). To do this we directly introduced the raw data into an open source estimation programme available on <https://www.estimationstats.com> (Ho et al., 2019) and downloaded the results and graphs. In this method each paired mean difference is plotted as a bootstrap sampling distribution, using 5000 bootstrap samples and the confidence intervals are bias-corrected and accelerated. The P value(s) reported are the likelihood(s) of observing the effect size(s), if the null hypothesis of zero difference is true. For each permutation P value, 5000 reshuffles of the control and test labels were performed. $P < 0.05$ is considered a significant difference.

Results

Recruiting C fibres does not change S1 local field evoked potential amplitudes at any age

Local field evoked potentials (EPs) were elicited in S1 at P7, P14, P21 and P30 (young adult) in response to electrical stimulation of the contralateral hindpaw. Stimuli were applied at strengths that activate only A fibres or both A+C fibres (10 stimuli at 10sec ISI, 3.2 mA, 50 μ s (A) or 500 μ s (A+C), n = 6 at each age) (Figure 1A). There was no significant difference between A fibre and A+C fibre EP peak amplitudes or onset latencies within each age (Figure 1B&C).

Recruiting C fibres adds a distinct, age related component to S1 oscillatory activity

Even if local field evoked potentials following A and A+C do not differ in the time domain, there still may be differences in the frequency content of the evoked activity which are not phase-locked to the stimulus and are therefore lost in the time average. To address this point, we compared the energy changes (relative to baseline) in the 1500ms epoch following A fibre and A+C fibre hindpaw stimulation.

Figure 2 shows the total energy change following hindpaw stimulation, relative to baseline, at each age. At P7 there is a large increase in energy which is restricted to the first 500 ms post-stimulus. From P14 onwards the energy changes, relative to baseline, are smaller but last for 1500ms. When total S1 oscillatory energy evoked by A fibre and by A+C fibre stimulation were directly compared, it was clear that A+C fibre evoked total energy is only significantly greater than A fibre at P30 in the 500-1000ms post-stimulus time epoch, with no significant differences in total energy attributable to C fibre recruitment before that age (Figure 2).

We next tested which frequency bands were contributing to the total energy differences between A and A+C fibres stimulation in Figure 2. To do this, we compared A and A+C energy changes within the same animal, in each frequency band: delta (2-4 Hz), theta (5-7 Hz), alpha (8-12 Hz), beta (15-29 Hz), gamma (30-90 Hz). Data was expressed as the paired difference between A+C fibre evoked energy and A fibre evoked energy at 0-500ms, 500-1000ms and 1000-1500ms post stimulus, at each age. The data was analysed using estimation statistics with a permutation t-test (Ho et al., 2019).

The main contribution to the energy difference at P30 500-1000 ms following stimulation was a significant increase in the gamma band (paired mean diff. 3.0 [95.0%CI 0.78, 6.4], two-sided permutation t-test, $P < 0.001$). This increase in gamma energy was also accompanied by increases in alpha (paired mean diff. 2.4 [95.0%CI 0.83, 2.67], $P = 0.03$) and beta (paired mean diff. 1.7 [95.0%CI 1.78, 5.68], $P < 0.001$) band energies (Figure 3). Figure 4A is a sample trace of the oscillatory signals recorded from S1 in a P30 rat following A fibre and at A+C fibre stimulation and shows the increase in gamma, alpha and beta frequency energies caused by recruitment of C fibres. At younger ages, significant decreases in energy were associated with C fibre stimulation: at P7 in the alpha band at 500-1000ms (paired mean diff. -2.2, [95.0%CI -4.01, 0.78], $P = 0.06$), and at P21 in the beta band energy at 1000-1500 (paired mean diff. -0.67, [95.0%CI -1.23, 0.19], $P = 0.03$) (Figure 3). Those changes were not sufficient to cause a significant drop in overall energy (Figure 2).

Silencing C fibres confirms age-related C fibre driven gamma and beta oscillatory activity in S1

The results above suggest that a distinct pattern of synchronised neural oscillations in the S1 can be attributed to the recruitment of peripheral C fibres. To explore this further, and better understand the age-related changes, we selectively silenced afferent TRPV1 positive C fibres in the hindpaw at P14, P21 and P30 using the membrane impermeable sodium channel blocker QX-314 inserted into C fibre afferents via the TRPV1 channel pore (Binshtok et al., 2007; Puopolo et al., 2013). Effective silencing was confirmed in awake and anaesthetised rats at all ages by significant reduction in hindpaw noxious heat sensitivity and in noxious mechanical reflexes (see Methods). We first measured the effect of C fibre silencing upon the total oscillatory energy in the 1500ms following stimulation, by comparing the energy in each frequency band evoked before and after QX-314 administration at P14, P21 & P30. Figure 5 shows that the overall energy is significantly reduced by C fibre silencing at P30, but not at younger ages (two-way RM ANOVA: P30, $p_{\text{condition}} = 0.02$, $F_{(1, 5)} = 10.36$; P21, $p_{\text{condition}} = 0.12$, $F_{(1, 5)} = 3.426$; P14, $p_{\text{condition}} = 0.51$, $F_{(1, 5)} = 0.49$), even though peripheral C fibres had been effectively blocked at all ages (see Methods). C fibre silencing has no significant effect at P14 and P21.

We next tested which frequency bands were contributing to the total energy differences after C fibres silencing in Figure 5. To do this, we compared the energy changes following A+C stimulation after QX314 treatment with those before treatment, within the same animal, in each frequency band. Data was expressed as the paired difference between energy after and energy before QX314 at 0-500ms, 500-1000ms and 1000-1500ms post stimulus, at each age. The data was analysed using estimation statistics with a permutation t-test.

Significant decreases in energy occurred at P30, in both the 500-1000ms and the 1000-1500ms epochs, with the greatest decrease being in the gamma band (500-1000ms, paired mean diff. -2.86 [95.0%CI -3.96, -1.64], two-sided permutation t-test, $P < 0.001$; 1000-1500ms, paired mean diff. -1.3 [95.0%CI -2.00, -0.62], two-sided permutation t-test, $P = 0.03$). This is accompanied by a significant decrease in beta band energy (paired mean diff. -1.6 [95.0%CI -2.9, -0.66], $P = 0.06$) (Figure 6). Figure 4B is a sample trace of the oscillatory signals recorded from S1 in a P30 rat before and after QX314 treatment and shows the decrease in gamma and beta frequency energies caused by silencing C fibres.

At younger ages, no change in gamma energy was detected but at P21 a significant decrease in beta energy occurred in the first 500ms (paired mean diff. -1.2, [95.0%CI -2.76, -0.4], $P < 0.001$). No significant changes were detected following C fibre silencing at P14.

Discussion

Here we show that in the young adult rat, activation of peripheral cutaneous afferent A and C fibres evokes a distinct age-related oscillatory activity in S1, that differs from that evoked by activation of cutaneous afferent A fibres alone. This was demonstrated by two experiments, one which tested the effect of recruiting C fibres to the stimulation paradigm and one which tested the effect of silencing C fibres in the stimulation paradigm. The effect of recruiting C fibres was shown by the difference between S1 oscillatory activity evoked by peripheral A fibres only and that evoked by A+C fibre stimulation. This difference revealed long latency increases in power in the alpha, beta and gamma range at P30, which can be ascribed to the additional recruitment of C fibres over A fibres alone. The effect of C fibre silencing was shown by the difference between S1 oscillatory activity after and before QX-314/capsaicin treatment. This difference resulted in the loss of long latency gamma

334 and beta energy, which can be ascribed to the absence of C fibre driven activity. Alpha activity was
335 highly variable in the silencing experiment, and no significant change was observed.

336 The results also show that the segregation of A fibre and C fibre driven oscillatory activity in S1
337 emerges postnatally. Distinct C fibre driven gamma and beta oscillatory activity was only observed
338 between 3 and 4 weeks of age (P21-30); no distinct C fibre oscillatory activity was detected in S1 at
339 younger ages. This finding is consistent with the results from ECoG recording S1 in the awake, freely
340 moving rat pup, where no prolonged change in oscillatory energy occurred post skin-incision until
341 P21 (Chang et al., 2016). At P7, the youngest age investigated here, cutaneous C fibres central
342 terminals have grown into the dorsal horn but the maturation of functional synapses with dorsal horn
343 neurons is still taking place (Fitzgerald, 2005), shifting from predominantly A β and A δ fibres
344 innervation to include C fibres innervation (Fitzgerald and Jennings, 1999; Koch and Fitzgerald, 2013;
345 Park et al., 1999). In the following week, from P8-P14, C fibres evoke increasing spike activity in
346 dorsal horn neurons (Jennings and Fitzgerald, 1998), and brainstem nuclei (Schwaller et al., 2016).
347 The onset of C fibres mediated oscillatory activity in S1 might be expected to occur soon after and
348 the results here show that it is not detectable before P21-P30. The lack of distinct C fibre driven
349 activity cannot be simply ascribed to the immaturity of neurons in the rat S1 cortex as clear tactile
350 sensory evoked potentials and somatosensory maps can be detected from the end of the first
351 postnatal week (Khazipov et al., 2004; Minlebaev et al., 2011; Mitrukina et al., 2015). The delayed
352 appearance of distinct C fibre evoked encoding within the S1 oscillatory activity may reflect the
353 structural and functional maturation of activity dependent cortical connections over this critical time
354 period (Feldman and Brecht, 2005; Pan-Vazquez et al., 2020; Pinto et al., 2013), in addition to changes
355 in the dorsal horn and thalamus (Koch and Fitzgerald, 2013; Murata and Colonnese, 2019).

356 In these experiments we used local field potential recording to compare the effect of electrical
357 stimulation of cutaneous A and C fibres upon oscillatory activity in layer 5 of the hindpaw S1.
358 Selective activation of A and A+C fibres with electrical stimulation of different pulse width or current
359 intensity is a classical method in electrophysiology which is still commonly used (Fitzgerald, 1985;
360 Smith et al., 2020; Stanfa and Dickenson, 2004). Higher current intensities are required to excite
361 unmyelinated fibres than myelinated fibres, but because of the strength–duration characteristic of
362 nerve excitation, increasing the duration of a stimulus while keeping amplitude constant allowed us
363 to activate the C fibre component of a compound action potential (CAP), as confirmed by our previous
364 studies (Koch and Fitzgerald, 2014). The technique also allowed us to quantitatively distinguish
365 between A and C fibre evoked activity at different ages using QX-314 C fibre silencing (Binshtok et al.,
366 2007; Koch et al., 2012; Koch and Fitzgerald, 2014). Many natural physiological stimuli will activate
367 both afferent fibre populations, but here we observed the difference between the composite effect
368 of activating A and C fibres simultaneously vs A fibres alone, so it is the "additive" contribution of
369 the C fibres in a scenario where both A and C fibres have been engaged. Silencing the C fibres
370 revealed the effect of removing that additive contribution. Selective activation of C fibres alone
371 using optogenetics (Beaudry et al., 2017) would discount any interaction caused by simultaneous
372 stimulation of A and C fibres, if the same time locked frequency plots could be achieved at all ages.

373 The pattern of C fibre evoked gamma activity reported here is consistent with reports of gamma
374 oscillatory activity associated with noxious laser stimulation in humans and rats. Its latency of >
375 500ms post stimulus is consistent with the slow conduction velocity of C fibres. Pain-related gamma
376 oscillatory activity in the somatosensory S1 predicts pain sensitivity (Hauck et al., 2007; Heid et al.,
377 2020; Hu and Iannetti, 2019) and inducing gamma oscillations in S1 enhances nociceptive sensitivity
378 and induces aversive avoidance behavior (Tan et al., 2019). Furthermore, noxious laser evoked
379 spiking in superficial S1 interneurons has strong phase coherence with gamma oscillations in awake
380 rats (Yue et al., 2020). C fibre activity was also associated with increases in beta energy at >500ms

latency post stimulus. In human subjects noxious stimulus intensity is encoded by decreases of neuronal oscillations at alpha and beta frequencies in sensorimotor areas (Nickel et al., 2017) but the beta (20–30 Hz) oscillations observed in our study may be related to the gating of C fibre input. Recent optogenetic studies show that beta oscillations are generated in S1 by strong feedback from the secondary somatosensory thalamus, which contains subpopulations of neurons that are highly responsive to noxious stimuli (Zhang and Bruno, 2019). An in vivo study of anesthetized mice found that this thalamic input can enhance the responsiveness of L5 pyramidal neurons to sensory stimulation (Mease et al., 2016). Thus the appearance of C fibre driven beta oscillations might increase the salience of somatic sensory inputs, especially when combined with gamma oscillations (Whittington et al., 2018). Recruiting C fibres in our study also increased alpha band energy consistent with reports in mice with inflammatory pain showing elevated resting alpha as well as gamma activity (Tan et al., 2019), but alpha activity was not sensitive to C fibre silencing and is therefore not likely to be directly linked to C fibre inputs.

However, it is important to note that the oscillatory profile reported here is selective for C fibre afferent inputs, but not necessarily selective for pain. The electrical stimulation paradigm separates the two major afferent fibre groups, myelinated A fibres and unmyelinated C fibres, but does not separate nociceptive and non-nociceptive modalities. While the majority of rodent sensory C fibres are polymodal nociceptors, the fundamental driver of lasting, unpleasant pain (Chisholm et al., 2018), some plantar foot C fibres in rats are cold receptors (but not low threshold mechanoreceptors as in other skin regions); equally, many nociceptors are A δ fibres (Leem et al., 1993).

These experiments were performed under light inhalation anaesthesia as stimulation at intensities required to activate C fibres evokes strong reflex movements in awake animals that would confound the results and cause considerable stress. Importantly, peripheral afferent volleys, travelling through ascending tracts, are known to reach the primary somatosensory cortex under anaesthesia in man (where they are used to improve accuracy in neurosurgery) (Eseonu et al., 2017) and in adult and infant rats (Chang et al., 2016, 2015; Granmo et al., 2013; Kalliomäki et al., 1998, 1993; Schouenborg et al., 1986; Shaw et al., 2001). In rat pups isoflurane at 1.5% does not affect the amplitude or frequency content of the initial somatosensory potential evoked by whisker deflection, but suppresses the successive early gamma oscillations (EGO) and spindle bursts (Minlebaev et al., 2011; Sitdikova et al., 2014) which are the result of corticothalamic feedback loop synchronization. This suggests that isoflurane does not interfere with the arrival of the afferent volley to S1 but inhibits further cortical processing. This effect may also differ with age (Chang et al., 2015); indeed somatosensory and noxious evoked cortical activity in young animals is highly resistant to anaesthesia (Sitkova, 2015, Chang et al, 2016b), which may explain the very high oscillatory S1 energies, relative to baseline, recorded here at P7. Our data is presented as differences within the same aged animals under the same level of anaesthesia, rather than between ages, because of this possibility. While the implications of this data for cortical mechanisms of sensory perception are limited by the anaesthesia, this does not diminish the importance of the information on encoding of afferent volleys in S1.

This study may have implications for the development of human cortical somatosensory processing. Behavioural reflex recording in newborn infants reveal that ‘nociceptive’ reflexes are indistinguishable from those evoked by innocuous touch (Cornelissen et al., 2013; Fitzgerald et al., 1988). The human infant brain undergoes a transition in response to tactile and noxious stimulation from nonspecific, evenly dispersed neuronal bursts to modality-specific, localized, evoked potentials, suggesting that specific neural circuits necessary for discrimination between touch and nociception emerge from 35–37 weeks gestation (Fabrizi et al., 2011). The emergence of the behavioural discrimination in early human life coincides with the brain responses discriminating noxious and

innocuous events (Green et al., 2019), suggesting a potential mechanistic link. By term, distinct BOLD activity patterns can be measured in response to different modalities and intensities of skin sensory stimulation in infants (Williams et al., 2015), but comparison of EEG responses to the same time-locked noxious skin lance revealed distinct differences in adult and infant oscillatory activity still remain (Fabrizi et al., 2016). This is consistent with the results of the current study where a direct and systematic measure of selective C fibre afferent encoding in rat S1 cortex is shown to change with age.

In conclusion, the results show that peripheral C fibre activity modulates oscillatory energy in the young adult rat S1, producing a distinct signature of increased beta and gamma rhythms, not observed following A fibre stimulation alone. Furthermore, it demonstrates the prolonged postnatal maturation of C fibre afferent coding in the mammalian brain.

References

- Baccei ML, Fitzgerald M (2013) Development of Pain Pathways and Mechanisms In: Wall & Melzack's Textbook of Pain (McMahon SB, Koltzenburg M, Tracey I, Turk D eds), pp143–155. Elsevier.
- Baccei ML, Fitzgerald M (2004) Development of GABAergic and glycinergic transmission in the neonatal rat dorsal horn. *J Neurosci* 24:4749–4757.
- Baccei ML, Fitzgerald M, Fitzgerald M (2003) Development of nociceptive synaptic inputs to the neonatal rat dorsal horn: glutamate release by capsaicin and menthol. *J Physiol (Lond)* 549:231–242.
- Beaudry H, Daou I, Ase AR, Ribeiro-da-Silva A, Séguéla P (2017) Distinct behavioral responses evoked by selective optogenetic stimulation of the major TRPV1+ and MrgD+ subsets of C-fibers. *Pain* 158:2329–2339.
- Beggs S, Torsney C, Drew LJ, Fitzgerald M (2002) The postnatal reorganization of primary afferent input and dorsal horn cell receptive fields in the rat spinal cord is an activity-dependent process. *Eur J Neurosci* 16:1249–1258.
- Binshtok AM, Bean BP, Woolf CJ (2007) Inhibition of nociceptors by TRPV1-mediated entry of impermeant sodium channel blockers. *Nature* 449:607–610.
- Bruns A (2004) Fourier-, Hilbert- and wavelet-based signal analysis: are they really different approaches? *Journal of Neuroscience Methods* 137:321–332.
- Chang P, Fabrizi L, Olhede S, Fitzgerald M (2016) The Development of Nociceptive Network Activity in the Somatosensory Cortex of Freely Moving Rat Pups. *Cereb Cortex* 26:4513–4523.
- Chang P, Walker SM, Fitzgerald M (2015) Neonatal rat primary somatosensory cortical pain activity is resistant to isoflurane anesthesia. *Anesthesiology*.
- Chisholm KI, Khovanov N, Lopes DM, La Russa F, McMahon SB (2018) Large Scale In Vivo Recording of Sensory Neuron Activity with GCaMP6. *eNeuro* 5.
- Coggeshall RE, Jennings EA, Fitzgerald M (1996) Evidence that large myelinated primary afferent fibers make synaptic contacts in lamina II of neonatal rats. *Brain Res Dev Brain Res* 92:81–90.
- Cornelissen L, Fabrizi L, Patten D, Worley A, Meek J, Boyd S, Slater R, Fitzgerald M (2013) Postnatal Temporal, Spatial and Modality Tuning of Nociceptive Cutaneous Flexion Reflexes in Human Infants. *PLoS One* 8.
- Eseonu CI, Rincon-Torroella J, ReFaey K, Lee YM, Nangiana J, Vivas-Buitrago T, Quiñones-Hinojosa A (2017) Awake Craniotomy vs Craniotomy Under General Anesthesia for Periolandic Gliomas: Evaluating Perioperative Complications and Extent of Resection. *Neurosurgery* 81:481–489.
- Fabrizi L, Slater R, Worley A, Meek J, Boyd S, Olhede S, Fitzgerald M (2011) A Shift in Sensory Processing that Enables the Developing Human Brain to Discriminate Touch from Pain. *Current Biology* 21:1552–1558.
- Fabrizi L, Verriotis M, Williams G, Lee A, Meek J, Olhede S, Fitzgerald M (2016) Encoding of mechanical nociception differs in the adult and infant brain. *Sci Rep* 6:28642.
- Feldman DE, Brecht M (2005) Map Plasticity in Somatosensory Cortex. *Science* 310:810–815.
- Fitzgerald M (2005) The development of nociceptive circuits. *Nature Reviews Neuroscience* 6:507–520.
- Fitzgerald M (1985) The post-natal development of cutaneous afferent fibre input and receptive field organization in the rat dorsal horn. *J Physiol (Lond)* 364:1–18.

- 478 Fitzgerald M, Jennings E (1999) The postnatal development of spinal sensory processing. *Proc Natl Acad Sci*
479 USA 96:7719–7722.
- 480 Fitzgerald M, Shaw A, MacIntosh N (1988) Postnatal development of the cutaneous flexor reflex:
481 comparative study of preterm infants and newborn rat pups. *Dev Med Child Neurol* 30:520–526.
- 482 Fransen AMM, Dimitriadis G, van Ede F, Maris E (2016) Distinct α - and β -band rhythms over rat
483 somatosensory cortex with similar properties as in humans. *J Neurophysiol* 115:3030–3044.
- 484 Granmo M, Jensen T, Schouenborg J (2013) Nociceptive transmission to rat primary somatosensory cortex--
485 comparison of sedative and analgesic effects. *PLoS ONE* 8:e53966.
- 486 Granmo M, Petersson P, Schouenborg J (2008) Action-based body maps in the spinal cord emerge from a
487 transitory floating organization. *J Neurosci* 28:5494–5503.
- 488 Green G, Hartley C, Hoskin A, Duff E, Shriver A, Wilkinson D, Adams E, Rogers R, Moultrie F, Slater R (2019)
489 Behavioural discrimination of noxious stimuli in infants is dependent on brain maturation. *Pain*
490 160:493–500.
- 491 Hauck M, Lorenz J, Engel AK (2007) Attention to Painful Stimulation Enhances γ -Band Activity and
492 Synchronization in Human Sensorimotor Cortex. *J Neurosci* 27:9270–9277.
- 493 Heid C, Mouraux A, Treede R-D, Schuh-Hofer S, Rupp A, Baumgärtner U (2020) Early gamma-oscillations as
494 correlate of localized nociceptive processing in primary sensorimotor cortex. *J Neurophysiol*.
- 495 Ho J, Tumkaya T, Aryal S, Choi H, Claridge-Chang A (2019) Moving beyond P values: data analysis with
496 estimation graphics. *Nat Methods* 16:565–566.
- 497 Hu L, Iannetti GD (2019) Neural indicators of perceptual variability of pain across species. *Proc Natl Acad Sci*
498 USA 116:1782–1791.
- 499 Jennings E, Fitzgerald M (1998) Postnatal changes in responses of rat dorsal horn cells to afferent
500 stimulation: a fibre-induced sensitization. *J Physiol (Lond)* 509 (Pt 3):859–868.
- 501 Kalliomäki J, Luo XL, Yu YB, Schouenborg J (1998) Intrathecally applied morphine inhibits nociceptive C fiber
502 input to the primary somatosensory cortex (SI) of the rat. *Pain* 77:323–329.
- 503 Kalliomäki J, Weng HR, Nilsson HJ, Schouenborg J (1993) Nociceptive C fibre input to the primary
504 somatosensory cortex (SI). A field potential study in the rat. *Brain Res* 622:262–270.
- 505 Khazipov R, Sirota A, Leinekugel X, Holmes GL, Ben-Ari Y, Buzsaki G (2004) Early motor activity drives spindle
506 bursts in the developing somatosensory cortex. *Nature* 432:758–761.
- 507 Killackey HP (1973) Anatomical evidence for cortical subdivisions based on vertically discrete thalamic
508 projections from the ventral posterior nucleus to cortical barrels in the rat. *Brain Res* 51:326–331.
- 509 Koch SC, Fitzgerald M (2014) The selectivity of rostroventral medulla descending control of spinal sensory
510 inputs shifts postnatally from A fibre to C fibre evoked activity. *J Physiol (Lond)* 592:1535–1544.
- 511 Koch SC, Fitzgerald M (2013) Activity-dependent development of tactile and nociceptive spinal cord circuits.
512 *Ann NY Acad Sci* 1279:97–102.
- 513 Koch SC, Tochiki KK, Hirschberg S, Fitzgerald M (2012) C-fiber activity-dependent maturation of glycinergic
514 inhibition in the spinal dorsal horn of the postnatal rat. *Proc Natl Acad Sci USA* 109:12201–12206.
- 515 Le Van Quyen M, Foucher J, Lachaux J, Rodriguez E, Lutz A, Martinerie J, Varela FJ (2001) Comparison of
516 Hilbert transform and wavelet methods for the analysis of neuronal synchrony. *J Neurosci Methods*
517 111:83–98.
- 518 Leem JW, Willis WD, Chung JM (1993) Cutaneous sensory receptors in the rat foot. *J Neurophysiol* 69:1684–
519 1699.
- 520 Minlebaev M, Colonnese M, Tsintsadze T, Sirota A, Khazipov R (2011) Early Gamma Oscillations Synchronize
521 Developing Thalamus and Cortex. *Science* 334:226–229.
- 522 Mitrukhina O, Suchkov D, Khazipov R, Minlebaev M (2015) Imprecise Whisker Map in the Neonatal Rat Barrel
523 Cortex. *Cereb Cortex* 25:3458–3467.
- 524 Murata Y, Colonnese MT (2019) Thalamic inhibitory circuits and network activity development. *Brain Res*
525 1706:13–23.
- 526 Nickel MM, May ES, Tiemann L, Schmidt P, Postorino M, Ta Dinh S, Gross J, Ploner M (2017) Brain oscillations
527 differentially encode noxious stimulus intensity and pain intensity. *Neuroimage* 148:141–147.
- 528 Pan-Vazquez A, Wefelmeyer W, Gonzalez Sabater V, Neves G, Burrone J (2020) Activity-Dependent Plasticity
529 of Axo-axonic Synapses at the Axon Initial Segment. *Neuron* 106:265-276.e6.

- 530 Park JS, Nakatsuka T, Nagata K, Higashi H, Yoshimura M (1999) Reorganization of the primary afferent
531 termination in the rat spinal dorsal horn during post-natal development. *Brain Res Dev Brain Res*
532 113:29–36.
- 533 Peng W, Tang D (2016) Pain Related Cortical Oscillations: Methodological Advances and Potential
534 Applications. *Front Comput Neurosci* 10.
- 535 Peng W, Xia X, Yi M, Huang G, Zhang Z, Iannetti G, Hu L (2018) Brain oscillations reflecting pain-related
536 behavior in freely moving rats. *Pain* 159:106–118.
- 537 Pfurtscheller G, Lopes da Silva FH (1999) Event-related EEG/MEG synchronization and desynchronization:
538 basic principles. *Clin Neurophysiol* 110:1842–1857.
- 539 Pinto JGA, Jones DG, Murphy KM (2013) Comparing development of synaptic proteins in rat visual,
540 somatosensory, and frontal cortex. *Front Neural Circuits* 7.
- 541 Puopolo M, Binshtok AM, Yao G-L, Oh SB, Woolf CJ, Bean BP (2013) Permeation and block of TRPV1 channels
542 by the cationic lidocaine derivative QX-314. *J Neurophysiol* 109:1704–1712.
- 543 Schouenborg J, Kalliomäki J, Gustavsson P, Rosén I (1986) Field potentials evoked in rat primary
544 somatosensory cortex (SI) by impulses in cutaneous A beta- and C-fibres. *Brain Res* 397:86–92.
- 545 Schwaller F, Kanellopoulos AH, Fitzgerald M (2017) The developmental emergence of differential brainstem
546 serotonergic control of the sensory spinal cord. *Sci Rep* 7:2215.
- 547 Schwaller F, Kwok C, Fitzgerald M (2016) Postnatal maturation of the spinal-bulbo-spinal loop: brainstem
548 control of spinal nociception is independent of sensory input in neonatal rats. *Pain* 157:677–686.
- 549 Shaw FZ, Chen RF, Yen CT (2001) Dynamic changes of touch- and laser heat-evoked field potentials of
550 primary somatosensory cortex in awake and pentobarbital-anesthetized rats. *Brain Res* 911:105–
551 115.
- 552 Sitdikova G, Zakharov A, Janackova S, Gerasimova E, Lebedeva J, Inacio AR, Zaynutdinova D, Minlebaev M,
553 Holmes GL, Khazipov R (2014) Isoflurane suppresses early cortical activity. *Annals of Clinical and*
554 *Translational Neurology* 1:15–26.
- 555 Smith TM, Lee D, Bradley K, McMahon SB (2020) Methodology for quantifying excitability of identified
556 projection neurons in the dorsal horn of the spinal cord, specifically to study spinal cord stimulation
557 paradigms. *J Neurosci Methods* 330:108479.
- 558 Stančák A (2006) Cortical oscillatory changes occurring during somatosensory and thermal stimulation In:
559 *Progress in Brain Research, Event-Related Dynamics of Brain Oscillations* (Neuper C, Klimesch W
560 eds), pp237–252. Elsevier.
- 561 Stanfa LC, Dickenson AH (2004) In vivo electrophysiology of dorsal-horn neurons. *Methods Mol Med* 99:139–
562 153.
- 563 Tadel F, Baillet S, Mosher JC, Pantazis D, Leahy RM (2011) Brainstorm: A User-Friendly Application for
564 MEG/EEG Analysis [WWW Document]. *Computational Intelligence and Neuroscience*. URL
565 <https://www.hindawi.com/journals/cin/2011/879716/> (accessed 1.13.20).
- 566 Tan LL, Oswald MJ, Heintz C, Retana Romero OA, Kaushalya SK, Monyer H, Künér R (2019) Gamma oscillations
567 in somatosensory cortex recruit prefrontal and descending serotonergic pathways in aversion and
568 nociception. *Nat Commun* 10:983.
- 569 Walker SM, Meredith-Middleton J, Lickiss T, Moss A, Fitzgerald M (2007) Primary and secondary hyperalgesia
570 can be differentiated by postnatal age and ERK activation in the spinal dorsal horn of the rat pup.
571 *Pain* 128:157–168.
- 572 Welker C (1971) Microelectrode delineation of fine grain somatotopic organization of (Sml) cerebral
573 neocortex in albino rat. *Brain Res* 26:259–275.
- 574 Whittington MA, Traub RD, Adams NE (2018) A future for neuronal oscillation research. *Brain Neurosci Adv*
575 2:2398212818794827.
- 576 Williams G, Fabrizi L, Meek J, Jackson D, Tracey I, Robertson N, Slater R, Fitzgerald M (2015) Functional
577 magnetic resonance imaging can be used to explore tactile and nociceptive processing in the infant
578 brain. *Acta Paediatr* 104:158–166.
- 579 Yue L, Iannetti GD, Hu L (2020) The Neural Origin of Nociceptive-Induced Gamma-Band Oscillations. *J*
580 *Neurosci* 40:3478–3490.

581 Zhang W, Bruno RM (2019) High-order thalamic inputs to primary somatosensory cortex are stronger and
582 longer lasting than cortical inputs. *Elife* 8.
583

584 Figure Legends

585
586 **Figure 1. Maturation of evoked local field potentials (EPs) in S1 following contralateral hindpaw stimulation. (A)**
587 Average EPs following A fibre (50µs) and A+C fibre (500µs) electrical stimulation of the contralateral hindpaw at P7,
588 P14, P21, and P30 (mean ± SEM, 10 stimuli at 10sec ISI, 3.2 mA, n = 6 rats at each age). Lower panels are a zoom-in view
589 of the grey boxes in the top panels. Vertical dotted lines indicate the time of stimulation. **(B)** EP peak amplitude and
590 **(C)** onset latency in response to electrical skin stimulation. (2-way mixed ANOVA, **= $p < 0.01$, ****= $p < 0.0001$, and
591 ns=not significant).

592 **Figure 2. Maturation of total energy changes in neuronal oscillations in S1 following contralateral hindpaw skin**
593 **stimulation.** Total energy changes evoked by A fibre (50µs) and A+C fibre (500µs) electrical stimulation of the
594 contralateral hindpaw at P7, P14, P21, and P30 between 0-500, 500-1000 and 1000-1500 ms post-stimulation. Mean (±
595 SEM) total energy changes (compared to baseline) following electrical stimuli (10 stimuli at 10sec ISI, 3.2 mA, n = 6 rats
596 at each age). Each dot represents the average across stimuli for each rat. Two-way RM ANOVA (summary results are
597 shown on top left of each panel) with Sidak's multiple comparisons test. *= $p < 0.05$; **= $p < 0.01$, ***= $p < 0.001$,
598 ****= $p < 0.0001$, and ns=not significant).

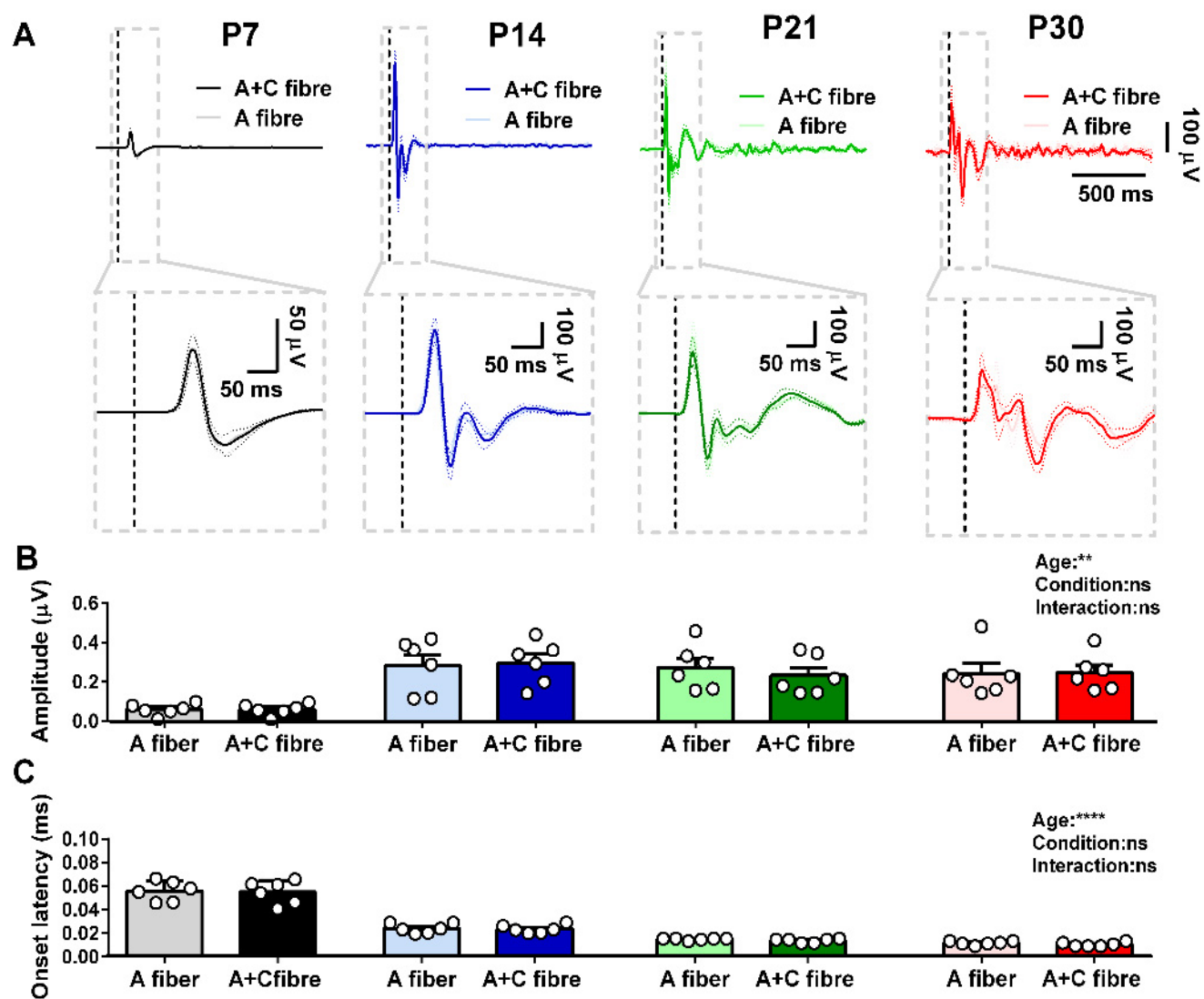
599 **Figure 3. Recruitment of cutaneous C fibres evokes distinct age-related increases in S1 gamma, beta and alpha**
600 **oscillatory energy.** Differences in the energy evoked by A+C fibre vs A fibre cutaneous stimulation in S1 at P7, P14, P21
601 & P30 (n=6 animals per age). The paired mean difference at 500-1000 and 1000-1500 ms post stimulus are shown for
602 each frequency band (delta (2-4 Hz), theta (5-7 Hz), alpha (8-12 Hz), beta (15-29 Hz), and gamma (30-90 Hz)). Mean
603 differences are depicted as dots; 95% confidence intervals are indicated by the ends of the vertical error bars. A positive
604 value means indicates a greater energy following A+C fibre stimulation, compared to A fibre stimulation and can be
605 attributed to recruitment of C fibres. Significant increases in gamma, alpha and beta energy occur at P30, and a significant
606 decrease in beta energy occurs at P21. A shorter latency (0-500ms) decrease in alpha energy at P7 is not shown. See
607 text for effect sizes, confidence intervals and permutation P values. Each paired mean difference is plotted as a bootstrap
608 sampling distribution, using 5000 bootstrap samples and the confidence intervals were bias-corrected and accelerated
609 (Ho et al., 2019).

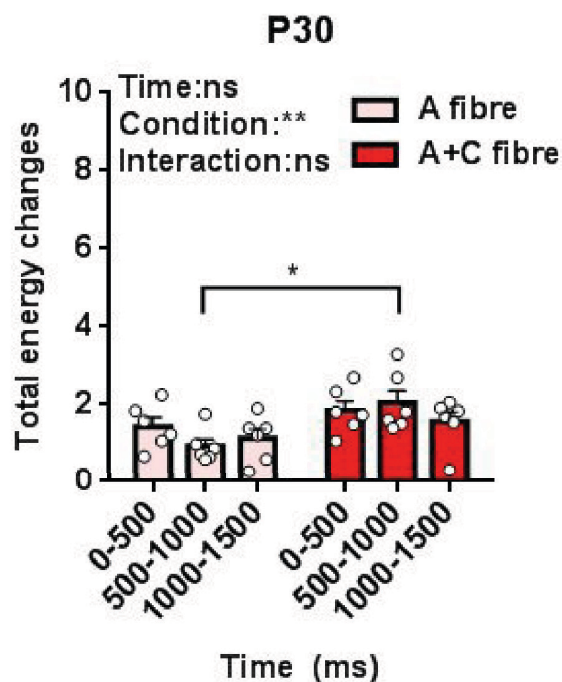
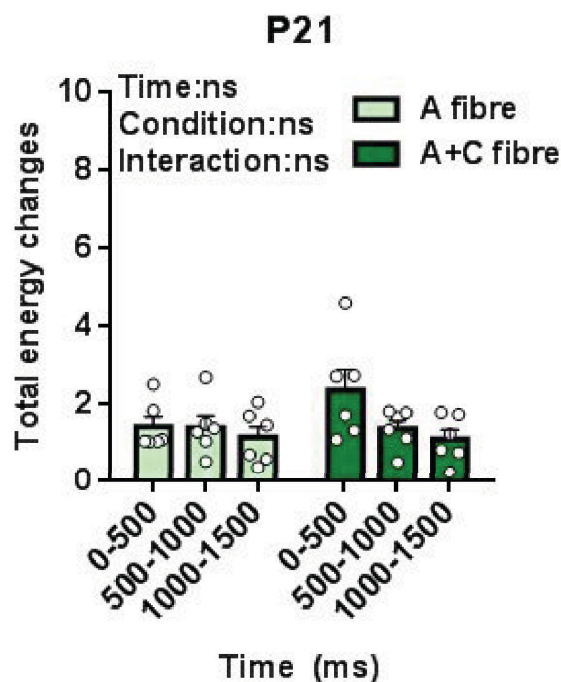
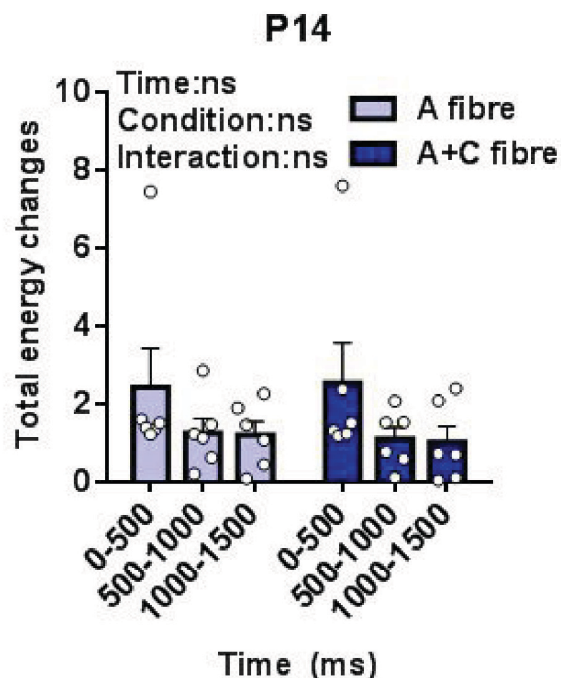
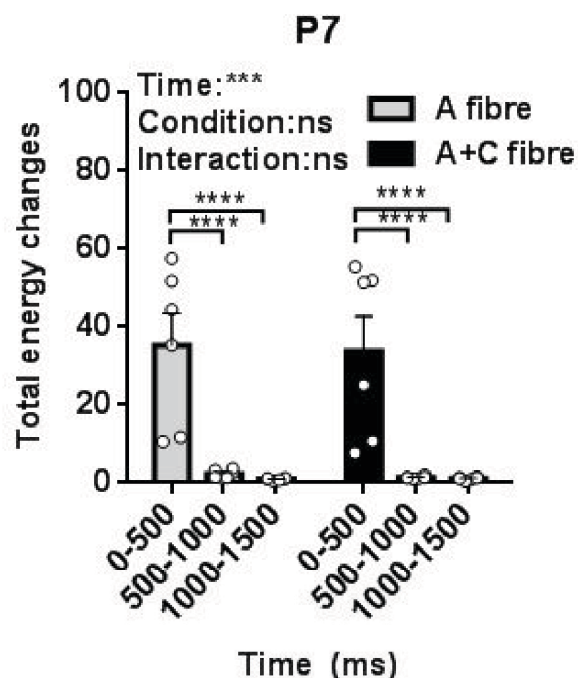
610 **Figure 4.** Sample raw traces of single EPs in P30 rat S1, following stimulation of the contralateral hindpaw, filtered to
611 display the contribution from five frequency bands. **A.** Stimulation at A fibre strength (left) and A+C fibre strength
612 (right). **B.** Stimulation before (left) and after QX314 treatment (right).

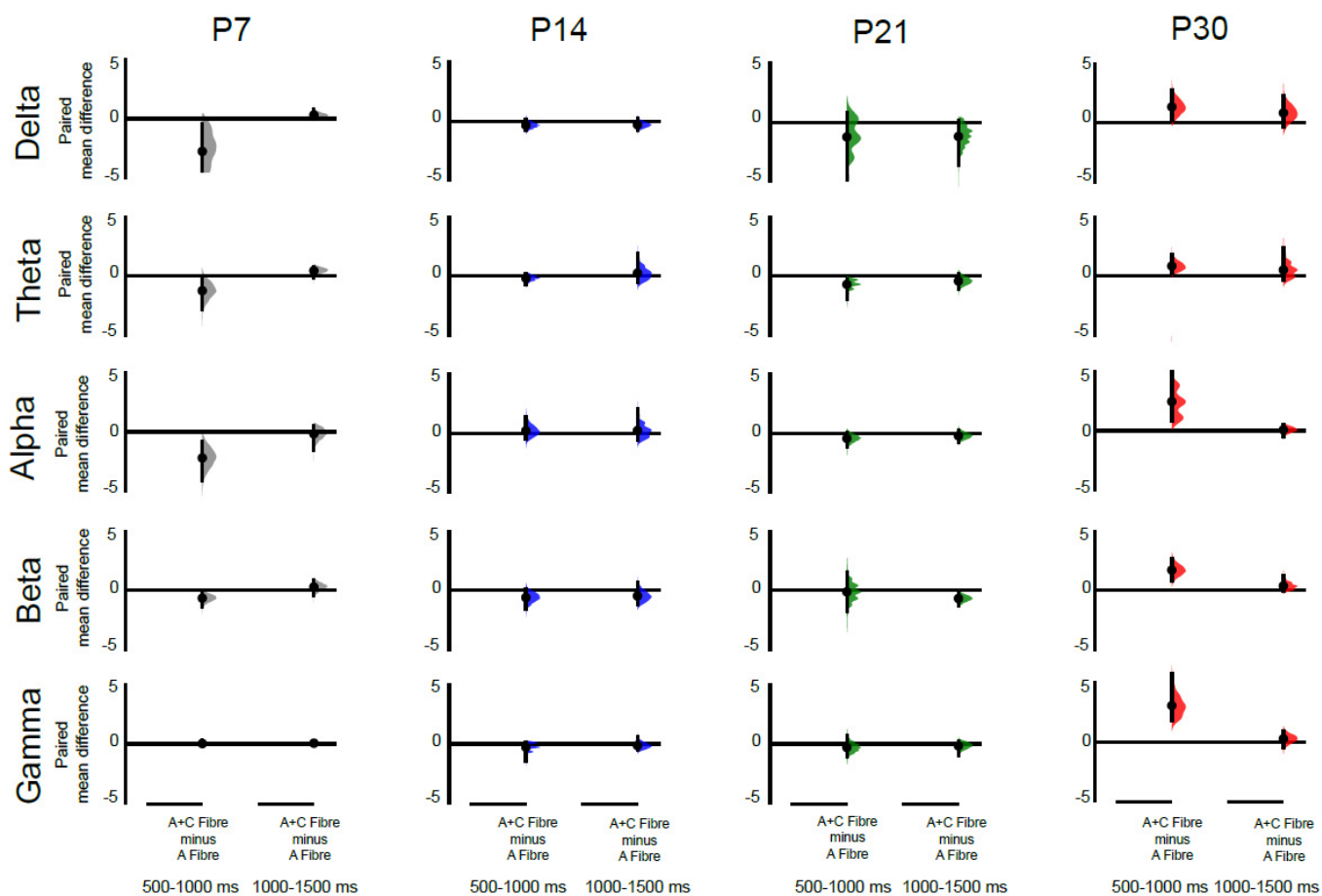
613 **Figure 5. Developmental regulation of total energy changes in S1 neuronal oscillations following C fibre silencing.**
614 Total energy changes evoked by A+C fibre (500µs) electrical stimulation of the contralateral hindpaw at P14, P21, and
615 P30 between 0-500, 500-1000 and 1000-1500 ms post-stimulation before and after silencing C fibres input. Mean (±
616 SEM) total energy changes (compared to baseline) to electrical stimuli (10 stimuli at 10sec ISI, 3.2 mA, n = 6 rats at each
617 age). Each dot represents the average across stimuli for each rat. Statistical analysis was performed using two-way RM
618 ANOVA (summary result is shown on top left of each panel) with Sidak's multiple comparisons test (significant between
619 groups were indicated by brackets). *= $p < 0.05$; **= $p < 0.01$, and ns=not significant).

620 **Figure 6. Silencing cutaneous C fibres causes distinct age-related decreases in S1 gamma and beta oscillatory energy.**
621 Differences in the energy evoked by stimulation after QX314 treatment vs before treatment in P14, P21 & P30 S1 (n=6
622 animals per age). The paired mean difference at 500-1000 and 1000-1500 ms post stimulus are shown for each frequency
623 band (delta (2-4 Hz), theta (5-7 Hz), alpha (8-12 Hz), beta (15-29 Hz), and gamma (30-90 Hz)). Mean differences are
624 depicted as dots; 95% confidence intervals are indicated by the ends of the vertical error bars. A negative value indicates
625 a decreased energy following QX treatment compared before treatment and can be attributed to silencing of C fibres.
626 Significant decreases in gamma and beta energy occur at P30. A decrease in beta energy at P21 at 0-500ms is not shown.
627 See text for effect sizes, confidence intervals and permutation P values. Each paired mean difference is plotted as a
628 bootstrap sampling distribution, using 5000 bootstrap samples and the confidence intervals were bias-corrected and
629 accelerated (Ho et al., 2019).
630

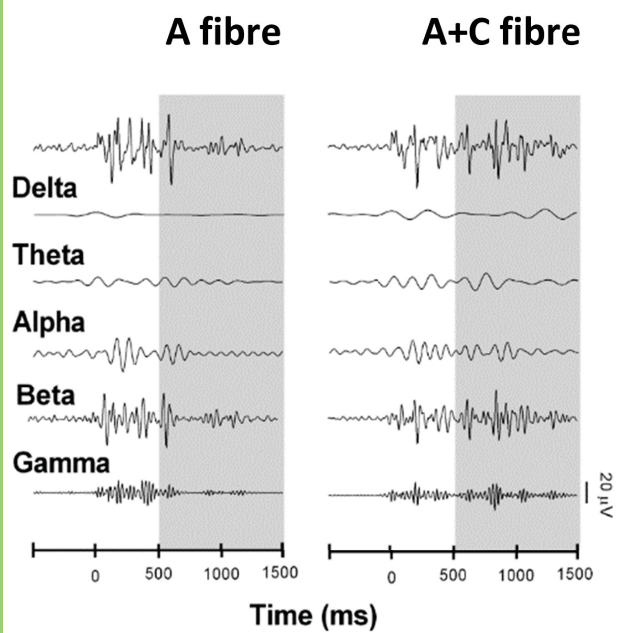
631







A



B

